



Development and validation of a four-microRNA signature for placenta accreta spectrum: an integrated competing endogenous RNA network analysis

Tian Yang^{1,2}, Na Li^{1,2}, Rui Hou^{1,2}, Chong Qiao^{1,2}, Caixia Liu^{1,2}

¹Department of Obstetrics and Gynecology, Shengjing Hospital of China Medical University, Shenyang, China; ²Key Laboratory of Maternal-Fetal Medicine of Liaoning Province, Key Laboratory of Obstetrics and Gynecology of Higher Education of Liaoning Province, Benxi, China

Contributions: (I) Conception and design: C Liu, C Qiao, T Yang; (II) Administrative support: C Liu, C Qiao; (III) Provision of study materials or patients: C Liu; (IV) Collection and assembly of data: N Li, T Yang; (V) Data analysis and interpretation: T Yang, R Hou; (VI) Manuscript writing: All authors; (VII) Final approval of manuscript: All authors.

Correspondence to: Chong Qiao; Caixia Liu. Department of Obstetrics and Gynecology, Shengjing Hospital of China Medical University, No.36 SanHao Street, HePing Area, Shenyang, China. Email: qiaochong2002@hotmail.com; liucxshimen@163.com.

Background: Placenta accreta spectrum (PAS) is a major cause of maternal morbidity and mortality in modern obstetrics, however, few studies have explored the underlying molecular mechanisms and biomarkers. In this study, we aimed to elucidate the regulatory RNA network contributing to PAS, comprising long non-coding (lnc), micro (mi), and messenger (m) RNAs, and identify biomarkers for the prediction of intraoperative blood volume loss.

Methods: Using RNA sequencing, we compared mRNA, lncRNA, and miRNA expression profiles between five PAS and five normal placental tissues. Furthermore, the miRNA expression profiles in maternal plasma samples from ten PAS and ten control participants were assessed. The data and clinical information were analyzed using R language and GraphPad Prism 7 software.

Results: Upon comparing PAS and control placentas, we identified 8,806 lncRNAs, 128 miRNAs, and 1,788 mRNAs that were differentially expressed. Based on a lasso regression analysis and correlation predictions, we developed a competing endogenous (ce) RNA network comprising 20 lncRNAs, 4 miRNAs, and 19 mRNAs. This network implicated a reduced angiogenesis pathway in PAS, and correlation analyses indicated that two miRNAs (hsa-miR-490-3p and hsa-miR-133a-3p) were positively correlated to operation-related blood volume loss.

Conclusions: We identified a ceRNA regulatory mechanism in PAS, and two miRNAs that may potentially serve as biomarkers of PAS prognosis.

Keywords: Placenta accreta spectrum (PAS); competing endogenous RNA network; angiogenesis; biomarkers; prognosis

Submitted Feb 01, 2020. Accepted for publication Jul 10, 2020.

doi: 10.21037/atm-20-1150

View this article at: <http://dx.doi.org/10.21037/atm-20-1150>

Introduction

Placenta accreta spectrum (PAS) is a pathological condition of placentation, whereby the placental chorionic villi adhere abnormally to or invade the uterine wall (1,2). PAS has been classified into three categories by pathologists: placenta accreta, in which the villi simply adhere to the myometrium;

placenta increta, in which the villi invade the myometrium; and placenta percreta, in which the villi invade the full thickness of the myometrium (1,2).

The prevalence of PAS has increased in recent years, being 2–90 per 10,000 births (3), but, in the United States, it can be as high as 1 in 272 in women with birth-related

hospital discharge diagnosis (4). Differences in study populations and diagnostic criteria may account for this wide range.

The most common risk factors associated with the occurrence of PAS are a previous caesarean delivery and placenta previa (5). Several other risk factors have also been reported, including cryopreserved embryo transfer, older maternal age, prior uterine surgery, parity, a higher body mass index (BMI), tobacco use, coexisting hypertension or diabetes, elevated second-trimester levels of α -fetoprotein and β -human chorionic gonadotropin, and a previous retained placenta or placenta accreta (6-10).

PAS results in maternal morbidity and mortality, preterm birth, low birth weight, perinatal mortality, recurrent placenta accreta, uterine rupture, and postpartum haemorrhage in subsequent pregnancies (11-14). Given these adverse consequences, the perinatal diagnosis and different treatments for PAS have focused on improving perinatal and maternal outcomes. Based on the few studies that have examined the pathogenesis of PAS, it has been hypothesised that decidua basalis defects, excessive trophoblast invasion, and abnormal vascular neovascularisation are the primary factors contributing to this disorder (2).

MicroRNAs (miRNAs) are small non-coding RNA molecules (~22 nucleotides long) that suppress gene expression by binding to the 3' end of the untranslated region (3'-UTR) of target mRNAs (15). In addition to post-transcriptional repression, miRNAs can also communicate with various RNA species in the competing endogenous RNA (ceRNA) network via microRNA response elements (MREs) (16). However, although it has been reported that miR-34a, miR-29a/b/c, and miR-125a are significantly down-regulated in PAS (17-19), the mechanisms by which miRNAs might contribute to PAS pathogenesis have yet to be determined; thus, a panoramic study in terms of miRNA networks in PAS is required. This study aimed to construct a ceRNA regulatory network in PAS based on small RNA and long non-coding (lnc) RNA sequencing analyses.

We present the following article in accordance with the MDAR reporting checklist (available at <http://dx.doi.org/10.21037/atm-20-1150>).

Methods

Patients

Women from Shengjing Hospital, China Medical

University, Shenyang, Liaoning were recruited if they had been diagnosed with placenta previa complications based on ultrasonography, had a history of at least one previous caesarean section and had a pregnancy terminated by caesarean section.

Patients were excluded if any of the following criteria were applicable: multiple pregnancy, foetal anomalies, pre-term premature rupture of membranes, or infection and complications associated with any other obstetric diseases, such as thyroid dysfunction, hypertension, and gestational diabetes. All participants enrolled in this study provided written informed consent.

The participants were divided into either a PAS or control group according to a placenta combined with tightly connected uterus pathology examination after caesarean section. Those in the PAS group were diagnosed by pathologists. Ultimately, we enrolled 20 patients, of whom two underwent hysterectomy, one underwent "segmental" resection, and seven underwent forcible placental removal.

The study was conducted in accordance with the Declaration of Helsinki (as revised in 2013). The study was approved by institutional ethics board of Shengjing Hospital, China Medical University (NO.: No.2017PS317K and No.2017PS318K) and informed consent was taken from all the patients.

Collection of placental tissue and blood samples

Placental tissues from ten patients (five each from the PAS and control groups) were collected immediately after caesarean section. Maternal placental specimens containing villous and extravillous trophoblasts, the fibrinoid layer, and the basal plate layer were collected from PAS (where placental tissues were tightly connected to the uterus and also included basal plate myometrial fibres) and control groups. The collected samples were washed in normal saline to remove excess blood, immediately immersed in liquid nitrogen, and then transferred to a -80°C freezer. Blood samples from 20 patients (ten each from the PAS and control groups) were obtained before caesarean section and centrifuged at 1,000 rpm for 20 min within 2 h to obtain plasma, which was subsequently stored at -80°C . The specimen collection was approved by institutional ethics board of Shengjing Hospital.

Total RNA isolation and sequencing

Total RNA was isolated by BGI-tech Standard with strict

quality control at each step. Samples were sequenced using BGISEQ-500 technology (20,21) for small RNAs and Illumina HiSeq for lncRNAs.

Real-time PCR

Total RNA was extracted using RNAiso Plus (cat. no. 9108; TaKaRa, Beijing, China) according to the manufacturer's protocol and was reverse transcribed using a Mir-X miRNA First-Strand Synthesis Kit (cat. no. 638315; TaKaRa, Beijing, China). Quantification of miRNAs was completed using TB Green[®] Premix Ex TaqTM II (Tli RNaseH Plus; cat. no. RR820A; TaKaRa, Beijing, China). Samples were subjected to real-time PCR, with the U6 gene as an endogenous control for miRNA normalisation. To obtain miRNA fold-change values relative to U6 expression, we used the $\Delta\Delta C_t$ method for analysis of the real-time data.

Immunohistochemical staining

Paraffin-embedded tissue sections were immunohistochemically stained for CD31 (1:200, cat. no. 11265-1-AP; Proteintech, Wuhan, China) using a Streptavidin-biotin Detection System (Rabbit kit SP-9001; ZSGB, Beijing, China). Briefly, the paraffin-embedded tissue sections were deparaffinised, hydrated in a graded ethanol series, and quenched by antigen retrieval. After primary and secondary antibody incubations, the slide was finally incubated with diaminobenzidine (DAB; cat. no. ZLI-9018; ZSGB, Beijing, China) and counterstained with haematoxylin (cat. no. G#1080; Solarbio, Beijing, China) for 10 s. Immunohistochemical analysis was performed microscopically. The CD31-labelled microvessel density (MVD) was assessed and quantified according to following criteria (22): a positive result was defined as a brown-yellow staining of vascular endothelial cells and MVD was determined based on brown-yellow stained single endothelial cells or endothelial cell clusters that were clearly separate from adjacent microvessels and other connective tissue elements. Five discrete fields of view with the highest vascular density were selected for observation under high magnification ($\times 400$), and the mean value was taken as the MVD value. Blood vessels with thick smooth muscle walls and a diameter greater than eight red blood cells were excluded.

Bioinformatics analysis

Genes that were differentially expressed between the PAS

and control groups (based on the criteria of an absolute fold change greater than 2 and an adjusted P value of less than 0.001) were identified using the R package DEGseq (23). The ceRNA network was visualised using the R package ggalluvial (24). We used RNAhybrid (25), miRanda (26), or TargetScan (27) to predict the mRNA targets of miRNAs and Starbase (28) to predict the lncRNA targets of miRNAs. We used the Co-LncRNA website to facilitate analysis of the correlation between lncRNAs and mRNAs (29). The David website was used to evaluate the functional implications, including Gene Ontology (GO) and Kyoto Encyclopaedia of Genes and Genomes (KEGG) pathway analyses, associated with our ceRNA network (30). Gene set enrichment analysis (GSEA) and gene set variation analysis (GSVA) were carried out to determine the enrichment of specific gene sets (31,32). Functional gene sets were obtained from (<http://amigo.geneontology.org/amigo/landing>).

Statistical analysis

To identify potential miRNAs, we performed lasso regression. The Student's *t*-test was used to assess differences in the distribution in continuous data, or the Mann-Whitney U test if the data were not normally distributed. The chi-square test or Fisher exact test was used for categorical variables. Pearson and Spearman correlation analyses were conducted to determine correlations according to distribution of the data. All statistical analyses were performed using SPSS 24.0, GraphPad Prism 7 (GraphPad Software Inc, La Jolla, CA), and R (<https://www.r-project.org>) software. $P < 0.05$ was considered statistically significant in two-tailed tests.

Results

Sequence profiling identified the differential expression of lncRNAs, miRNAs, and mRNAs

In the present study, we identified 1,788 mRNAs (1,124 up-regulated and 664 down-regulated), 128 miRNAs (77 up-regulated and 51 down-regulated), and 8,806 lncRNAs (2,548 up-regulated and 6,258 down-regulated) that were differentially expressed between the PAS and control groups. The differentially expressed lncRNAs were defined and annotated using the Ensembl genome browser 96 (<http://asia.ensembl.org/index.html>), which resulted in a reduction in number to 913 (325 up-regulated and 588

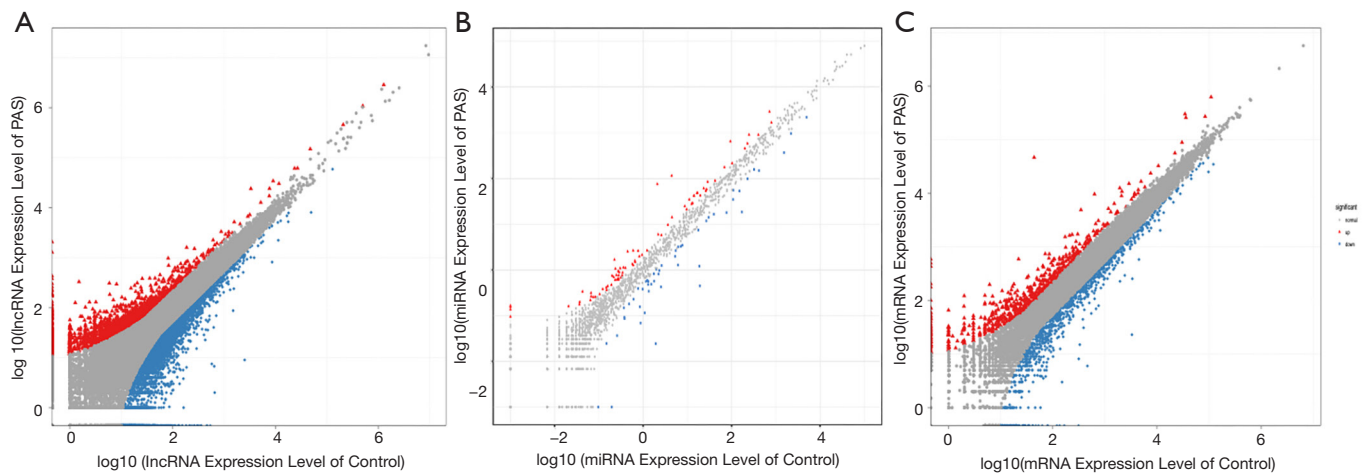


Figure 1 Plots showing the expression levels of long non-coding (lnc), micro (mi), and messenger (m) RNA genes. Panels (A,B,C) show the log₁₀-transformed expression of lncRNA, miRNA, and mRNA genes, respectively. Red triangles denote up-regulated genes, blue squares denote down-regulated genes, and grey dots denote non-regulated genes. PAS, placenta accreta spectrum.

down-regulated). To visualise the differences in lncRNAs, miRNAs, and mRNAs between the PAS and control groups, we constructed plots showing the respective gene expression levels (*Figure 1*).

Construction of a ceRNA network contributing to PAS

To identify the miRNAs implicated in PAS, we performed a lasso regression analysis of the differentially expressed miRNAs and accordingly identified the following seven miRNAs: hsa-miR-10524-5p, hsa-miR-133a-3p, hsa-miR-937-3p, hsa-miR-34b-5p, hsa-miR-3529-3p, hsa-miR-488-3p, and hsa-miR-490-3p (*Figure 2A,B*). We then predicted the target mRNAs of these seven miRNAs and intersected them with the differentially expressed mRNAs, from which we identified miRNA–mRNA interacting pairs involving four miRNAs and 65 mRNAs. Similarly, among the differentially expressed lncRNAs, we identified 33 that were predicted to interact with the four miRNAs. Given the positive correlation between lncRNAs and mRNAs in the ceRNA network, we performed correlation analysis to visualise the filtered lncRNAs–mRNAs (*Figure 2C*). As a result of this analysis, we obtained a ceRNA network comprising 43 unique RNAs (20 lncRNAs, four miRNAs, and 19 target mRNAs), as shown in *Figure 2D*.

The PAS group exhibited reduced angiogenesis signatures

To examine the biological features of the ceRNA network,

we performed GO and KEGG analyses, which revealed that the most relevant biological processes in PAS were angiogenesis-related processes with no enrichment in the KEGG pathway (*Figure 3A*). To further confirm the relationship between angiogenesis-related processes and PAS, we conducted GSEA based on 377 GO terms and found that angiogenesis-related processes, such as ‘Venous blood vessel development’, were, as expected, generally reduced in the PAS group (*Figure 3B*). Furthermore, we conducted GSEA of three main angiogenesis-related terms, ‘Angiogenesis’, ‘Blood vessel morphogenesis’, and ‘Placenta blood vessel development’, with the results showing that there was a significant negative enrichment of ‘Angiogenesis’ and ‘Blood vessel morphogenesis’, but no significant enrichment of ‘Placenta blood vessel development’, in the PAS group (*Figure 3C*, the data of ‘Placenta blood vessel development’ are not shown).

hsa-miR-490-3p and hsa-miR-133a-3p expression shows a positive correlation with blood volume loss

To clarify the relationship between the four miRNAs in the ceRNA network and operation-related blood volume loss, we performed plasma small RNA sequencing in 20 patients and subsequent correlation analyses. The clinical information is summarised in *Table 1*. We accordingly detected a significant difference in the intraoperative blood loss between the PAS and control groups (2,120.0±971.60 vs. 765.0±956.86 mL, P=0.006).

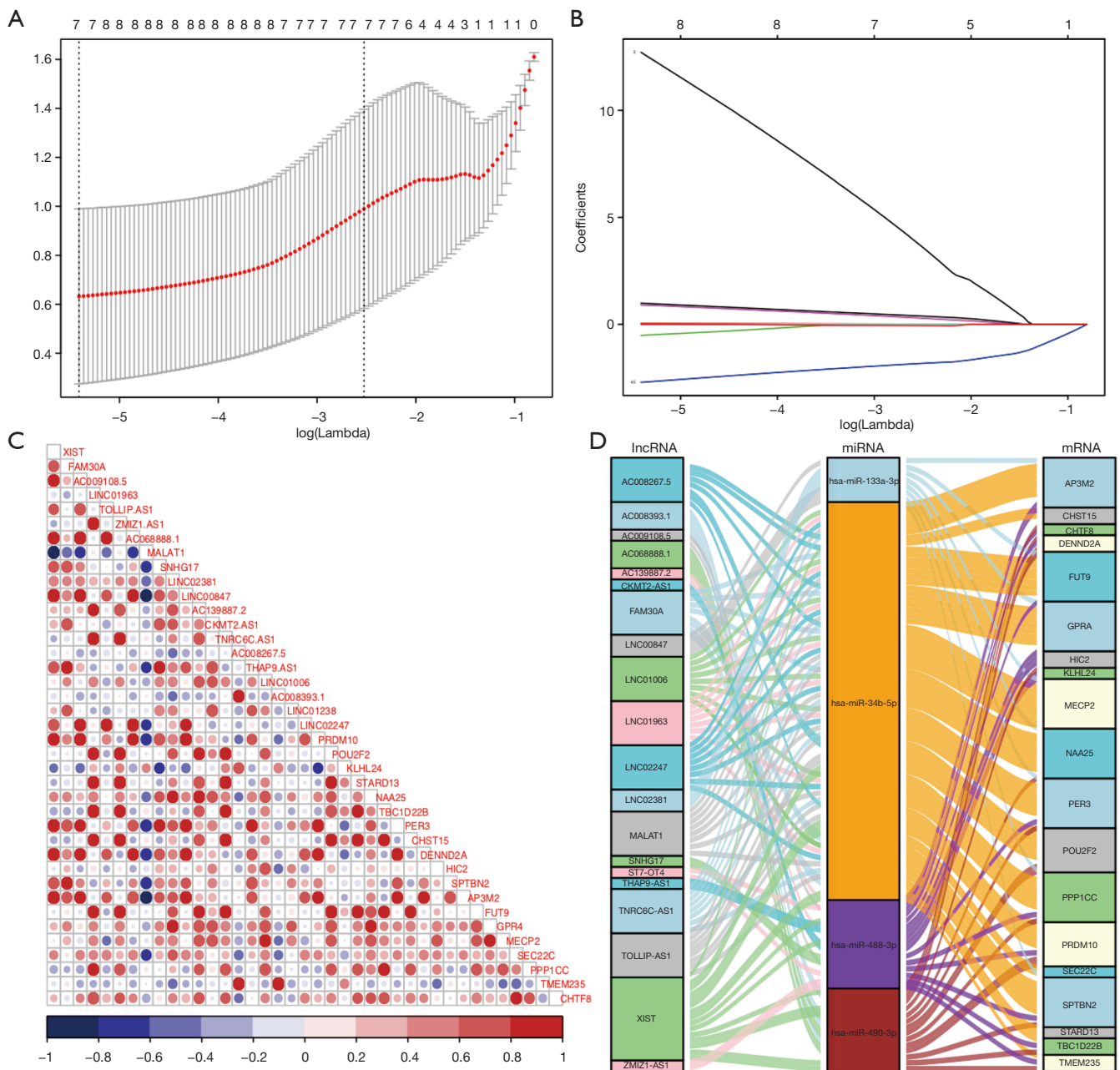


Figure 2 The competing endogenous (ce) RNA network. (A) Results of a lasso regression analysis of 128 differentially expressed miRNAs. Ten-fold cross-validation was used to calculate the best lambda value that leads to minimum mean cross-validated error. Red dots denote partial likelihood deviance; solid vertical lines indicate their corresponding 95% confidence intervals; the left dotted vertical line is the value of lambda that gives minimum cvm, denoted as lambda.min; and the right dotted vertical line is the largest value such that the error is within 1 standard error of the minimum, denoted as lambda.1se. (B) The coefficient values at varying levels of penalty. Each curve represents a miRNA. (C) The correlation between lncRNAs and mRNAs in the ceRNA network. Blue circles indicate a negative correlation and red circles indicate a positive correlation. (D) A Sankey diagram for the ceRNA network in placenta accreta spectrum. Left bar: lncRNA; middle bar: miRNA; right bar: mRNA. Each rectangle represents a gene, and the degree of connection of each gene is indicated by the size of the rectangle.

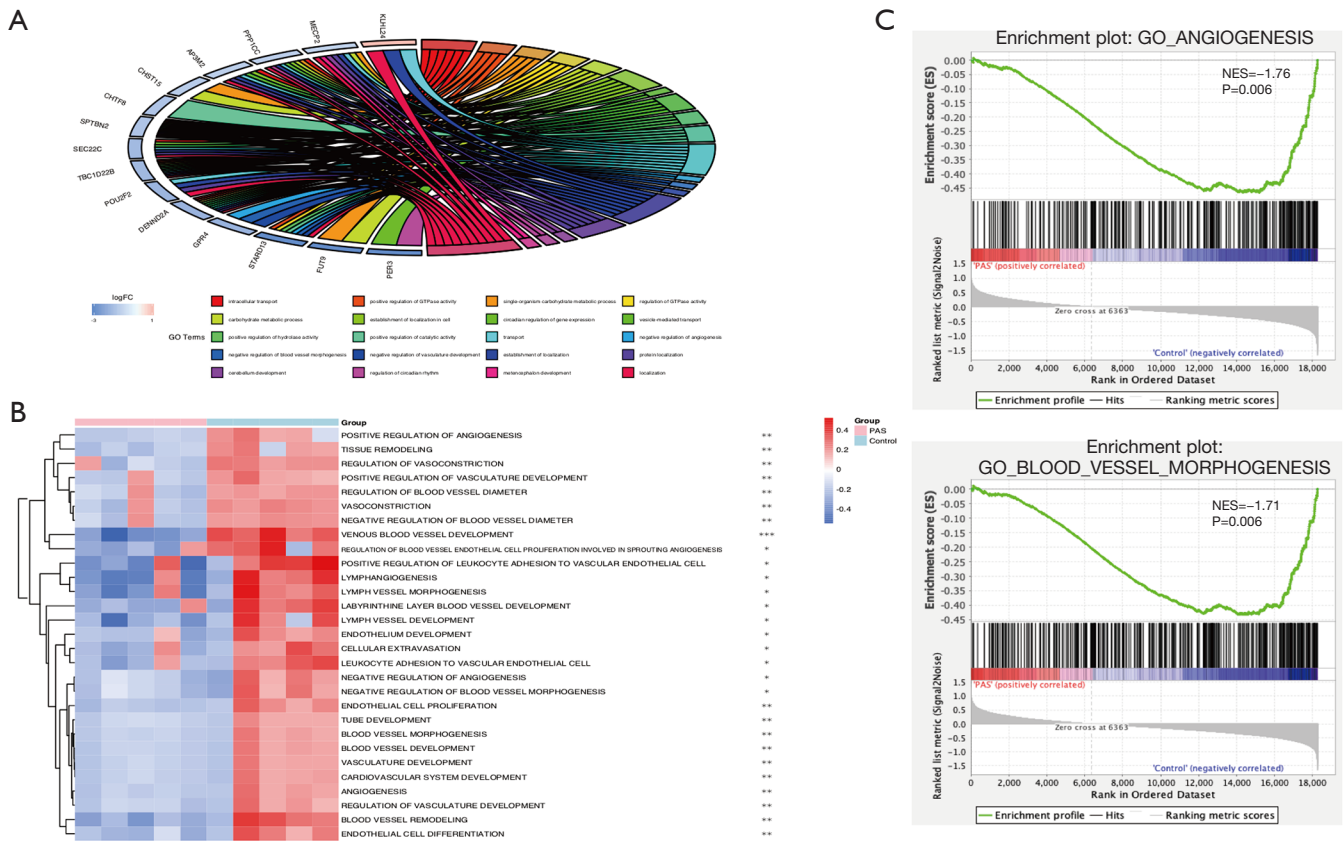


Figure 3 The competing endogenous RNA network has a reduced angiogenesis status. (A) The GO terms are defined as indicated colour bars at the bottom and shown in the bottom-right chord diagram. The involved differentially expressed mRNAs are shown at the bottom left. The red and blue bars represent up-regulated and down-regulated genes, respectively. (B) Gene set variation analysis results indicated that angiogenesis-related terms were enriched in control patients. (C) Gene set enrichment analysis results revealed that there was a negative enrichment of two angiogenesis-related terms ('Angiogenesis' and 'Blood vessel morphogenesis') in placenta accreta spectrum (PAS) patients. *, $P < 0.05$; **, $P < 0.01$; and ***, $P < 0.001$.

No differences, however, were observed between the two groups with regard to any other characteristics. The findings of the correlation analyses indicated that the expression of hsa-miR-490-3p and hsa-miR-133a-3p was positively correlated to operation-related blood volume loss, and the Pearson correlation coefficients were 0.603 ($P = 0.0049$, 95% CI: 0.212–0.825) and 0.5655 ($P = 0.0094$, 95% CI: 0.164–0.806) for miR-133a-3p and miR-490-3p, respectively (Figure 4, the data of miR-488-3p and miR-34b-5p are not shown).

RT-PCR results verified the validity of the identified ceRNAs and small RNA-sequencing

To further establish the validity of the aforementioned

results, we determined and analysed the expression levels of the four miRNAs involved in the ceRNA network. The results showed that the levels of hsa-miR-133a-3p, hsa-miR-488-3p, and hsa-miR-490-3p were significantly higher in PAS patients than in control patients ($P = 0.014$, 0.0002, and 0.0046, respectively); in contrast, the expression of hsa-miR-34b-5p was significantly lower ($P = 0.0494$). We also randomly selected five miRNAs (hsa-miR-193a-3p, hsa-miR-501-3p, hsa-miR-770-5p, hsa-miR-103a-3p, and hsa-miR-137-3p) to validate the results of small RNA-sequencing (Figure 5A), and, accordingly, found that the results obtained from RT-qPCR validation were completely consistent with those obtained from bioinformatics analyses.

Table 1 Demographic and obstetric characteristics of selected enrolled patients

Characteristics	PAS (n=10)	Control (n=10)	P value
Age (years)	31.7±5.36	34.1±4.77	0.304
BMI	28.3±2.32	28.0±3.71	0.874
Gravity	3.5 [2–7]	3 [2–5]	0.436
Parity	1 [1–2]	1 [1–2]	0.739
Number of CSs	1 [1–2]	1 [1–1]	0.739
Number of artificial abortions	1 [0–2]	0.5 [0–3]	0.579
Gestational weeks	36.2±0.65	36.6±0.74	0.303
Intraoperative blood loss	2120.0±971.60	765.0±956.86	0.006

Values are presented as the mean ± standard deviation (SD) and median (range). PAS, placenta accreta spectrum; BMI, body mass index; CS, caesarean section.

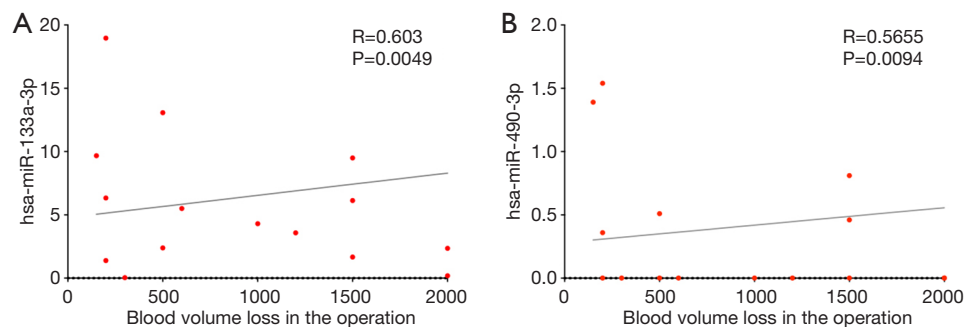


Figure 4 The relationship between the four miRNAs in the competing endogenous RNA network and intraoperative blood volume loss. We detected positive correlations between intraoperative blood volume loss and the expression of miR-133a-3p and miR-490-3p in the maternal plasma; the Pearson correlation coefficients were 0.603 ($P=0.0049$, 95% CI: 0.212–0.825) and 0.5655 ($P=0.0094$, 95% CI: 0.164–0.806) for miR-133a-3p and miR-490-3p, respectively. CI, confidence interval.

Immunohistochemical staining

To confirm the reduced angiogenesis function in PAS, we performed immunohistochemical analysis using the vessel endothelial cell marker CD31, which revealed reduced immunoreactivity in PAS associated with a greater number of larger blood vessels and reduced microvessel density (Figure 5B,C). The results accordingly confirmed the function of the ceRNA network.

Discussion

In this study, we developed a ceRNA regulatory network in PAS and determined that the expression of the miRNAs hsa-miR-490-3p and hsa-miR-133a-3p is positively correlated with operation-related blood volume loss.

miRNAs play a critical role in placental development (33–35), and, although a few studies have examined RNA expression profiles in severe preeclampsia, early pregnancy loss, and foetal growth restriction (36–40), no studies, to the best of our knowledge, have sought to identify the miRNA expression profiles in PAS. Here, we found that the expression of the miRNAs miR-490-3p, miR-133a-3p, miR-488-3p, and miR-34b-5p differed between the PAS and control groups based on small RNA expression profile. Abundant evidence indicates that these four miRNAs serve as tumour suppressors in cancers (41–44). Interestingly, we found that, whereas the expression levels of miR-490-3p, miR-133a-3p, and miR-488-3p were higher in the PAS group, those of miR-34b-5p were lower. The four miRNAs might regulate different or same mRNAs to promote the development of PAS. Decreased miR-34b-

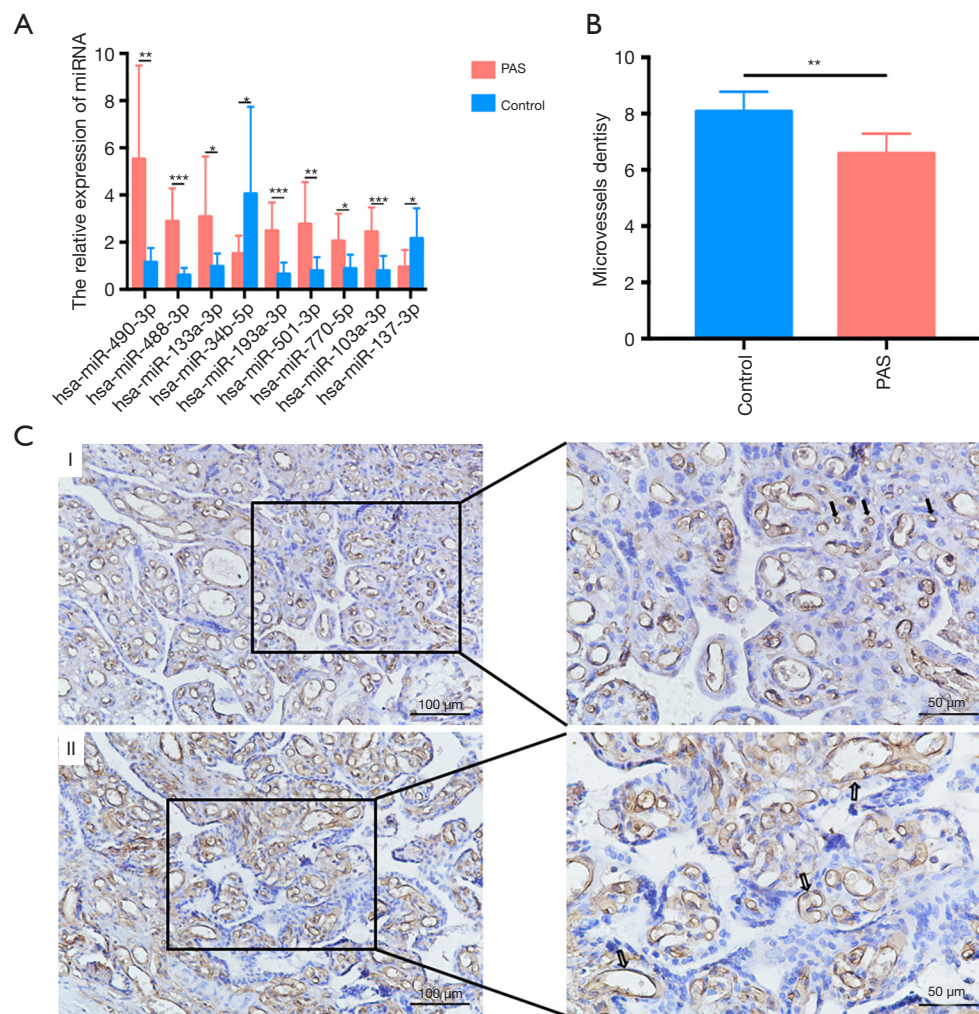


Figure 5 Validation of the RNA-sequencing and biological function of the competing endogenous RNA network. (A) The RT-PCR results showed that the expression of miR-490-3p, miR-488-3p, miR-133a-3p, miR-193a-3p, miR-501-3p, miR-770-5p, and miR-103a-3p was higher in the placenta accreta spectrum (PAS) group than in the control group, whereas that of miR-34b-5p and miR-137-3p was decreased. These results were consistent with those of RNA-sequencing; (B) compared with that in the control group, the PAS group exhibited lower microvessel density; (C) immunohistochemical staining of the vessel endothelial cell marker CD31: (I) represents the control group and (II) represents the PAS group. In each case, the left- and right-hand panels show vessels at $\times 200$ and $\times 400$ magnification, respectively. Solid and hollow arrows indicate microvessels and macrovessels, respectively. The control group showed a larger number of microvessels, whereas the PAS group showed a larger number of macrovessels. *, $P < 0.05$; **, $P < 0.01$; and ***, $P < 0.001$.

5p could promote proliferation and differentiation, inhibit apoptosis and increase migration of trophoblasts, leading to PAS. Of course, we must note that the expression levels of miR-490-3p, miR-133a-3p and miR-488-3p were elevated and might inhibit the biological function of trophoblasts. Nevertheless, we suspect that miR-34b-5p may play the most important role in trophoblasts among these miRNAs. Moreover, although several studies have reported that

these three miRNAs are tumour suppressors in cancers, we cannot suggest that they similarly affect trophoblasts at the maternal-foetal interface. At the same time, the general role of miRNAs involves a negative feedback regulation; however, there is also an involvement of positive regulation. Therefore, the mechanism by which these four miRNAs affect the development of PAS still needs further exploration.

To clarify the biological implications of the expression of these four miRNAs in PAS, we constructed a ceRNA network, which indicated that the angiogenesis pathway was repressed in the PAS group. In this regard, although increasing evidence has indicated the role of trophoblast invasion and decidua basalis defects in PAS, few studies have focused on abnormal vascular neovascularisation. In the present study, we detected reduced angiogenesis in the placenta of PAS patients. Consistently, results obtained based on GSEA, GSVA, and immunohistochemical staining revealed a decrease in MVD in PAS. Previous studies have reported the expression levels of angiogenic and anti-angiogenic factors in the placenta and serum of PAS patients. For example, Tseng *et al.* reported an increase and decrease in the expression levels of VEGF and sVEGFR-2, respectively, in tissues from PAS (45), whereas Wehrum *et al.* (46) and Uyanıkoğlu *et al.* (47) have demonstrated significant decreases in the maternal circulatory levels of VEGF. Moreover, Uyanıkoğlu *et al.* (47) also found that the levels of sFlt-1 and placental growth factor were lower. Lower expression of sFlt-1 in PAS has also been reported by other groups (48,49), whereas Duzyj *et al.* (50) found increased levels of intervillous Eng in PAS. Given the differences in enrolment criteria, time of sample collection, and types of samples, there is still a lack of consensus regarding the expression patterns of angiogenic and anti-angiogenic factors in tissues and maternal plasma, and, thus, their precise functional role remains to be clarified.

Nevertheless, despite the current uncertainty in this regard, it is generally accepted that extensive neovascularisation is a prominent feature in the majority of PAS cases (51). Previously, Chantraine *et al.* reported that vessels were significantly larger and sparser in the PAS placental beds (52), which is consistent with the findings of the present study. Placental angiogenesis commences from day 32 of gestation, when hemangioblasts derived from extraembryonic mesoderm allantois differentiate into endothelial cells (53). Subsequent formation of multi-branched capillary networks is characterised by branching angiogenesis prior to 24 weeks post-conception, and thereafter non-branching angiogenesis continues to term (54). Given the reduced number of microvessels detected in the present study, we speculate that sprouting and intussusceptive angiogenesis are suppressed in PAS patients, resulting in fewer but larger vessels, which is similar to clinical ultrasound findings. However, in view of the fact that samples were collected from the third trimester in the present study, we cannot exclude the

possibility that our results simply reflect the conditions at term, and the true state in the first and second trimesters remains unknown. We speculated that extensive neovascularization might occur during the first and second trimesters, however, further investigations are required. In our previous study, we detected high expression levels of VEGF in PAS placentas (55), which might reflect a compensatory increase in response to reduced angiogenesis.

Haemorrhage during or after an operation is considered a major complication of PAS, and, in the present study, we found there was a significant difference in the intraoperative blood loss between the PAS and control groups. Moreover, the expression of miR-490-3p and miR-133a-3p in maternal plasma was found to be positively correlated with intraoperative blood loss. We thus propose that, in the future, it might be possible to predict the amount of intraoperative blood loss in patients with PAS-related complications by determining the expression levels of miR-490-3p and miR-133a-3p in maternal plasma, which can lead to preventive measure to reduce blood loss and improve the prognosis of mother and child. Moreover, the two miRNAs miR-490-3p and miR-133a-3p could be deemed as suitable biomarkers to predict the probability of PAS by sampling plasma in early pregnancy.

To our knowledge, this is the first study to examine the regulatory network comprising lncRNAs, miRNAs, and mRNAs in PAS and identify biomarkers for the prediction of intraoperative blood volume loss. In addition, we demonstrated the importance of angiogenesis in PAS.

However, we acknowledge that this study has certain limitations, notably that our findings are based on a small number of samples and that there was a lack of samples from the early trimester, particularly from the maternal plasma. Regardless, the small sample size might be indicative of the overall incidence of PAS in pregnancy and the current diagnostic criteria based on pathological examination. Future large-scale studies that include the analysis of maternal plasma collected during the first or second trimester must be performed. Moreover, the molecular mechanisms underlying the activities of the four miRNAs involved in the ceRNA network and the prognostic value of miR-490-3p and miR-133a-3p should be fully investigated.

Conclusions

In the present study, we identified a ceRNA regulatory mechanism in PAS, and identified the miRNAs miR-490-3p

and miR-133a-3p as biomarkers with potential prognostic value.

Acknowledgments

Funding: The study was supported by the Ministry of Science and Technology of the People's Republic of China (No. 2016YFC100404 to CQ), and the Liaoning Provincial Education Department (No. LS201611 for NL).

Footnote

Reporting Checklist: The authors have completed the MDAR checklist. Available at <http://dx.doi.org/10.21037/atm-20-1150>

Data Sharing Statement: Available at <http://dx.doi.org/10.21037/atm-20-1150>

Conflicts of Interest: All authors have completed the ICMJE uniform disclosure form (available at <http://dx.doi.org/10.21037/atm-20-1150>). The authors have no conflicts of interest to declare.

Ethical Statement: The authors are accountable for all aspects of the work in ensuring that questions related to the accuracy or integrity of any part of the work are appropriately investigated and resolved. The study was conducted in accordance with the Declaration of Helsinki (as revised in 2013). The study was approved by institutional ethics board of Shengjing Hospital, China Medical University (NO.: No. 2017PS317K and No. 2017PS318K) and informed consent was taken from all the patients.

Open Access Statement: This is an Open Access article distributed in accordance with the Creative Commons Attribution-NonCommercial-NoDerivs 4.0 International License (CC BY-NC-ND 4.0), which permits the non-commercial replication and distribution of the article with the strict proviso that no changes or edits are made and the original work is properly cited (including links to both the formal publication through the relevant DOI and the license). See: <https://creativecommons.org/licenses/by-nc-nd/4.0/>.

References

1. Jauniaux E, Collins S, Burton GJ. Placenta accreta spectrum: pathophysiology and evidence-based anatomy for prenatal ultrasound imaging. *Am J Obstet Gynecol* 2018;218:75-87.
2. Jauniaux E, Jurkovic D. Placenta accreta: pathogenesis of a 20th century iatrogenic uterine disease. *Placenta* 2012;33:244-51.
3. Thurn L, Lindqvist PG, Jakobsson M, et al. Abnormally invasive placenta-prevalence, risk factors and antenatal suspicion: results from a large population-based pregnancy cohort study in the Nordic countries. *BJOG* 2016;123:1348-55.
4. Mogos MF, Salemi JL, Ashley M, et al. Recent trends in placenta accreta in the United States and its impact on maternal- fetal morbidity and healthcare-associated costs, 1998-2011. *J Matern Fetal Neonatal Med* 2016;29:1077-82.
5. Society of Gynecologic Oncology, American College of Obstetricians and Gynecologists and the Society for Maternal-Fetal Medicine, Cahill AG, et al. Placenta Accreta Spectrum. *Am J Obstet Gynecol* 2018;219:B2-16.
6. Jauniaux E, Bhide A. Prenatal ultrasound diagnosis and outcome of placenta previa accreta after cesarean delivery: a systematic review and meta-analysis. *Am J Obstet Gynecol* 2017;217:27-36.
7. Balayla J, Bondarenko HD. Placenta accreta and the risk of adverse maternal and neonatal outcomes. *J Perinat Med* 2013;41:141-9.
8. Mullen C, Battarbee AN, Ernst LM, et al. Occult Placenta Accreta: Risk Factors, Adverse Obstetrical Outcomes, and Recurrence in Subsequent Pregnancies. *Am J Perinatol* 2019;36:472-5.
9. Carusi DA. The Placenta Accreta Spectrum: Epidemiology and Risk Factors. *Clin Obstet Gynecol* 2018;61:733-42.
10. Kaser DJ, Melamed A, Bormann CL, et al. Cryopreserved embryo transfer is an independent risk factor for placenta accrete. *Fertil Steril* 2015;103:1176-84.e2.
11. Vinograd A, Wainstock T, Mazor M, et al. Placenta accrete is an independent risk factor for late pre-term birth and perinatal mortality. *J Matern Fetal Neonatal Med* 2015;28:1381-7.
12. Farquhar CM, Li Z, Lensen S, et al. Incidence, risk factors and perinatal outcomes for placenta accreta in Australia and New Zealand: a case-control study. *BMJ Open* 2017;7:e017713.
13. Kabiri D, Hants Y, Shanwetter N, et al. Outcomes of Subsequent Pregnancies After Conservative Treatment for Placenta Accreta. *Int J Gynaecol Obstet* 2014;127:206-10.
14. Eshkoli T, Weintraub AY, Sergienko R, et al. Placenta accreta: risk factors, perinatal outcomes,

- and consequences for subsequent births. *Am J Obstet Gynecol* 2013;208:219.e1-7.
15. Bartel DP. MicroRNAs: Genomics, biogenesis, mechanism and function. *Cell* 2004;116:281-97.
 16. Salmena L, Poliseno L, Tay Y, et al. A ceRNA hypothesis: the Rosetta Stone of a hidden RNA language? *Cell* 2011;146:353-8.
 17. Gu Y, Bian Y, Xu X, et al. Downregulation of miR-29a/b/c in placenta accreta inhibits apoptosis of implantation site intermediate trophoblast cells by targeting MCL1. *Placenta* 2016;48:13-9.
 18. Umemura K, Ishioka S, Endo T, et al. Roles of microRNA-34a in the pathogenesis of placenta accreta. *J Obstet Gynaecol Res* 2013;39:67-74.
 19. Gu Y, Meng J, Zuo C, et al. Downregulation of MicroRNA-125a in Placenta Accreta Spectrum Disorders Contributes Antiapoptosis of Implantation Site Intermediate Trophoblasts by Targeting MCL1. *Reprod Sci* 2019;26:1582-9.
 20. Wang Z, Gerstein M, Snyder M. RNA-Seq: a revolutionary tool for transcriptomics. *Nat Rev Genet* 2009;10:57-63.
 21. Mortazavi A, Williams BA, McCue K, et al. Mapping and quantifying mammalian transcriptomes by RNA-Seq. *Nature Methods* 2008;5:621-8.
 22. Weidner N, Folkman J, Pozza F, et al. Tumor angiogenesis: a new significant and independent prognostic indicator in early-stage breast carcinoma. *J Natl Cancer Inst* 1992;84:1875-87.
 23. Wang L, Feng Z, Wang X, et al. DEGseq: an R package for identifying differentially expressed genes from RNA-seq data. *Bioinformatics* 2010;26:136-8.
 24. Rosvall M, Bergstrom CT. Mapping change in large networks. *PLoS One* 2010;5:e8694.
 25. Krüger J, Rehmsmeier M. RNAhybrid: microRNA target prediction easy, fast and flexible. *Nucleic Acids Res* 2006;34:W451-4.
 26. John B, Enright AJ, Aravin A, et al. Human MicroRNA targets. *PLoS Biol* 2004;2:e363.
 27. Agarwal V, Bell GW, Nam J, et al. Predicting effective microRNA target sites in mammalian mRNAs. *eLife* 2015;4:e05005.
 28. Li JH, Liu S, Zhou H, et al. StarBase v2.0: decoding miRNA-ceRNA, miRNA-ncRNA and protein-RNA interaction networks from large-scale CLIP-Seq data. *Nucleic Acids Res* 2014;42:D92-7.
 29. Zhao Z, Bai J, Wu A, et al. Co-LncRNA: investigating the lncRNA combinatorial effects in GO annotations and KEGG pathways based on human RNA-Seq data. *Database (Oxford)* 2015;2015:bav082.
 30. X Jiao, BT Sherman, R Stephens, et al. DAVID-WS: a stateful web service to facilitate gene/protein list analysis. *Bioinformatics* 2012;28:1805-6.
 31. Hänzelmann S, Castelo R, Guinney J. GSEA: gene set variation analysis for microarray and RNA-seq data. *BMC Bioinformatics* 2013;14:7.
 32. Subramanian A, Tamayo P, Mootha VK, et al. Gene set enrichment analysis: a knowledge-based approach for interpreting genome-wide expression profiles. *Proc Natl Acad Sci U S A* 2005;102:15545-50.
 33. Farrokhnia F, Aplin JD, Westwood M, et al. MicroRNA Regulation of Mitogenic Signaling Networks in the Human Placenta. *J Biol Chem* 2014;289:30404-16.
 34. Hayder H, O'Brien J, Nadeem U, et al. MicroRNAs: crucial regulators of placental development. *Reproduction* 2018;155:R259-71.
 35. Vaiman D. Genes, epigenetics and miRNA regulation in the placenta. *Placenta* 2017;52:127-33.
 36. Choi SY, Yun J, Lee OJ, et al. MicroRNA expression profiles in placenta with severe preeclampsia using a PNA-based microarray. *Placenta* 2013;34:799-804.
 37. Gunel T, Hosseini MK, Gumusoglu E, et al. Expression profiling of maternal plasma and placenta microRNAs in preeclamptic pregnancies by microarray technology. *Placenta* 2017;52:77-85.
 38. Hosseini MK, Gunel T, Gumusoglu E, et al. MicroRNA expression profiling in placenta and maternal plasma in early pregnancy loss. *Mol Med Rep* 2018;17:4941-52.
 39. Higashijima A, Miura K, Mishima H, et al. Characterization of placenta-specific microRNAs in fetal growth restriction pregnancy. *Prenat Diagn* 2013;33:214-22.
 40. Yang S, Li H, Ge Q, et al. Deregulated microRNA species in the plasma and placenta of patients with preeclampsia. *Mol Med Rep* 2015;12:527-34.
 41. Maroof H, Islam F, Ariana A, et al. The roles of microRNA-34b-5p in angiogenesis of thyroid carcinoma. *Endocrine* 2017;58:153-66.
 42. Yin Y, Du L, Li X, et al. miR-133a-3p suppresses cell proliferation, migration, and invasion and promotes apoptosis in esophageal squamous cell carcinoma. *J Cell Physiol* 2019;234:12757-70.
 43. Leng K, Xu Y, Kang P, et al. Akirin2 is modulated by miR-490-3p and facilitates angiogenesis in cholangiocarcinoma through the IL-6/STAT3/VEGFA signaling pathway. *Cell Death Dis* 2019;10:262.

44. Yang Y, Li H, He Z, et al. MicroRNA-488-3p inhibits proliferation and induces apoptosis by targeting ZBTB2 in esophageal squamous cell carcinoma. *J Cell Biochem* 2019;120:18702-13.
45. Tseng JJ, Chou MM, Hsieh YT, et al. Differential expression of vascular endothelial growth factor, placenta growth factor and their receptors in placentae from pregnancies complicated by placenta accreta. *Placenta* 2006;27:70-8.
46. Wehrum MJ, Buhimschi IA, Salafia C, et al. Accreta complicating complete placenta previa is characterized by reduced systemic levels of vascular endothelial growth factor and by epithelial-to-mesenchymal transition of the invasive trophoblast. *Am J Obstet Gynecol* 2011;204:411.e1-11.
47. Uyanikoğlu H, İncebiyık A, Turp AB, et al. Serum Angiogenic and Anti-angiogenic Markers in Pregnant Women with Placenta Percreta. *Balkan Med J* 2018;35:55-60.
48. McMahan K, Karumanchi SA, Stillman IE, et al. Does soluble fms-like tyrosine kinase-1 regulate placental invasion? Insight from the invasive placenta. *Am J Obstet Gynecol* 2014;210:68.e1-4.
49. Shainker SA, Dannheim K, Gerson KD, et al. Down-regulation of soluble fms-like tyrosine kinase 1 expression in invasive placentation. *Arch Gynecol Obstet* 2017;296:257-62.
50. Duzyj CM, Buhimschi IA, Laky CA, et al. Extravillous trophoblast invasion in placenta accreta is associated with differential local expression of angiogenic and growth factors: a cross-sectional study. *BJOG* 2018;125:1441-8.
51. Bartels HC, Postle JD, Downey P, et al. Placenta Accreta Spectrum: A Review of Pathology, Molecular Biology, and Biomarkers. *Dis Markers* 2018;2018:1507674.
52. Chantraine F, Blacher S, Berndt S, et al. Abnormal vascular architecture at the placental-maternal interface in placenta increta. *Am J Obstet Gynecol* 2012;207:188.e1-9.
53. Kaufmann P, Mayhew TM, Charnock-Jones DS. Aspects of human fetoplacental vasculogenesis and angiogenesis. II. Changes during normal pregnancy. *Placenta* 2004;25:114-26.
54. Chen DB, Zheng J. Regulation of Placental Angiogenesis. *Microcirculation* 2014;21:15-25.
55. Li N, Yang T, Yu W, et al. The role of Zeb1 in the pathogenesis of morbidly adherent placenta. *Mol Med Rep* 2019;20:2812-22.

Cite this article as: Yang T, Li N, Hou R, Qiao C, Liu C. Development and validation of a four-microRNA signature for placenta accreta spectrum: an integrated competing endogenous RNA network analysis. *Ann Transl Med* 2020;8(15):919. doi: 10.21037/atm-20-1150